مجلة جامعة بني وليد للعلوم الإنسانية والتطبيقية
تصدر عن جامعة بني وليد – ليبيا
Website: https://jhas-bwu.com/index.php/bwjhas/index
المجلد التاسع، العدد الثالث الصفحات (614-631) 2024م

محاكاة عددية للموصلية الكهربائية للمركبات الهجينة العضوية وغير العضوية بواسطة النماذج القائمة على الذكاء الاصطناعي

مريم اخويطر[1]، إبراهيم حيدر[2]
[1]قسم الفيزياء، كلية الآداب والعلوم– المرج، جامعة بنغازي، بنغازي، ليبيا
[2]قسم الفيزياء، كلية التربية بالمرج، جامعة بنغازي، بنغازي، ليبيا
maryam.akhwater@uob.edu.ly

Numerical simulation for electrical conductivity of organic–inorganic hybrid compounds by artificial intelligence–based models

Maryam Akhwater [1], Ibrahim Haidr[2]
[1] Department of physics, Faculty of art and science– Almarj, University of Benghazi, Libya.
[2] Department of physics, Faculty of Education– Almarj, University of Benghazi, Libya

تاريخ الاستلام:03-08-2024 تاريخ القبول: 20-08-2024 تاريخ النشر: 04-09-2024

الملخص:

في هذا العمل، تم تطبيق الأساليب القائمة على الذكاء الاصطناعي للتنبؤ بالموصلية الكهربائية للمركبات الهجينة العضوية وغير العضوية، وهي **tritetrapropylammoniumdodeca chlorobismuthate(III)** $[(C_3H_7)_4N]_3Bi_3Cl_{12}$ و **bis (4-acetylaniline) tetrachlorocadmate** $[C8H10NO]2[CdCl4]$ بناءا على معرفة درجة حرارة النظام والتردد فقط. تم تدريب أساليب التعلم الآلي المقترحة واختبارها والتحقق من صحتها باستخدام مجموعات البيانات التجريبية التي تم نشرها مسبقا. تم استخدام مجموعات البيانات هذه كمدخلات لخوارزميات التعلم الآلي المختلفة؛ هذه الخوارزميات المنفذة هي الشبكة العصبية الاصطناعية ذات التدرج المترافق **(ANN-SCG)**، و الشبكة العصبية الاصطناعية ذات الانحدار المتدرج **(ANN-GD)**، بالإضافة الي شجرة القرار. على وجه الخصوص، تم تحسين جميع نماذج الشبكات العصبية الاصطناعية عن طريق تعزيز المعاملات الفائقة للشبكات من أجل إنتاج بنية شبكية عصبية فائقة، والتي توفر أدنى قيمة لخطأ التدرج. عند المقارنة، وجد أن جميع نماذج الشبكات العصبية الاصطناعية أظهرت دقة متناهية في إظهار العلاقات غير الخطية مع مجموعة بيانات الموصلية الكهربائية، مما أدى إلى تنبؤ أفضل بالموصلية الكهربائية المحاكاة بدقة تزيد عن 99٪ لمجموعات البيانات المدخلة. لم يتمكن نموذج شجرة القرار من التنبؤ بالموصلية الكهربائية بدقة مقبولة من حيث قيم ***RMSEs*** العالية ومعاملات الارتباط المنخفضة. استناداً إلى النتائج التي تم الحصول عليها، تؤكد الدراسة على أن الشبكات العصبية

الاصطناعية تمثل تقنيات فعالة للغاية للتنبؤ بالارتباطات غير الخطية والمعقدة بين المتغيرات المستقلة ومعامل الاستجابة التابع.

الكلمات الدالة: الشبكة العصبية الاصطناعية (**ANN**)، الذكاء الاصطناعي، شجرة القرار، الموصلية الكهربائية، النمذجة، المركبات العضوية و غير العضوية.

Abstract

In this work, artificial intelligence-based approaches were applied to predict the electrical conductivity for organic-inorganic hybrid compounds, namely tritetrapropylammoniumdodeca chlorobismuthate(III) $[(C_3H_7)_4N]_3Bi_3Cl_{12}$ and bis (4-acetylaniline) tetrachlorocadmate $[C8H10NO]2[CdCl4]$ with only the knowledge of the system temperature and frequency. The suggested machine learning methods are trained, tested, and validated using experimental datasets. These datasets were used as inputs to different machine learning algorithms; these implemented algorithms are artificial neural network-scaled conjugate gradient (ANN-SCG), artificial neural network-gradient descent (ANN-GD), and decision tree. In particular, all ANN models were optimised by adjusting the hyperparameters in order to produce a superior neural network architecture, which provides the lowest value of the gradient error. Upon comparison, it was found that all ANN models showed better accuracy and significant precision in demonstrating nonlinear relationships with the electrical conductivity dataset, leading to a better prediction of the simulated electrical conductivity with more than 99% accuracy for the presented data sets. The decision tree model could not predict the electrical conductivity with acceptable accuracy in terms of high *RMSEs* and low correlation coefficients. Based on the obtained results, it suggested that ANNs were quite efficient techniques for predicting nonlinear and complicated correlations between independent variables and the response parameter.

Keywords: Artificial Neural Network (ANN), Artificial-intelligence, Decision tree, Electrical conductivity, Modelling, Organic-inorganic compounds.

INTRODUCTION

Over the past few years, a heterostructure of organic-inorganic materials in one compound has attracted increasing attention due to their outstanding structural, electronic, optical, thermal, magnetic, and catalytic properties. In general, the properties of these materials can be controlled to fit a specific application as they link strongly to their structural variations under several synthesis process parameters such as temperature and chemical composition. Organic materials have several p-type semiconductors that can be fabricated by cost-effective growth methods [1, 2, 3]. In particular, these materials have superior light absorption, making them a great candidate for solar cells, photodetectors, and light-emitting diodes (LEDs) [4, 5, 6]. Even though organic materials can provide high fluorescence capacity, broad polarizability, and structural diversity, they yet undergo some challenges, such as poor carrier mobility, low

thermodynamic stability, disorganized growth on some traditional substrates such as SiO_2, and less carrier injection, which still needs to be addressed [7, 8, 9]. Therefore, the focus of scientific research is to combine organic and inorganic heterostructures in one product to enhance the current multifunctional devices and broaden their efficiencies by exploiting the excellent properties of both materials. Thus, inorganic materials with significant carrier mobility and ultra-flatness dangling bond-free interface can perform as promising substrates to synthesize higher-quality organic materials with sharp-edged interfaces, which offer excellent charge transportation pathways for producing high-efficiency electronic and optoelectronic devices [10]. Besides, organic materials as large tunable light absorbers can enhance the efficiency of 2-dimensional transition metal dichalcogenides (TMDCs) based photodetectors by expanding their spectral detectivity level with large responsivity and ultrafast charge carrier dissociation [11, 12, 13]. In addition, organic materials can serve as a superior alternative for solar cell applications by boosting carrier mobility for FETs [14, 15], accelerating charge carrier dissociation and slowing down reconnection of organic–inorganic heterostructure [16, 17]. Therefore, organic–inorganic hybrid compounds have paved the way for a broad spectrum of novel applications in optoelectronics [18], p-n junctions [19], catalysis [20], photovoltaics [21], and neuromorphic computing devices [22]. It reported that the electrical characteristics of most organic–inorganic hybrid compounds can be studied by evaluating their electrical conductivity, which is mostly utilized to understand the electrical conduction behaviour of solid-state materials [23]. Therefore, this work aims to apply several predictive algorithms, namely, SCG-ANN, GD-ANN, and decision tree, to predict the electrical conductivity of two different organic-inorganic hybrid compounds, which are $[(C_3H_7)_4N]_3Bi_3Cl_{12}$ and [C8H10NO]2[CdCl4]. In addition, the performance and accuracy of all proposed models were validated as anticipation approaches through analytical methodology, and the connections between the input and output parameters were confirmed.

Artificial intelligence-based models

In general, artificial intelligence-based models are innovative algorithms that analyse datasets with accuracy, determine complicated patterns, and enable the system to produce sensible decisions. These sophisticated artificial intelligence algorithms perform according to a concept of machine learning and are designed to simulate human brain intelligence. They learn from profound training datasets to build their insight and predictive potencies. In addition, it reported that artificial intelligence techniques show better performance compared to conventional statistics for modelling complex nonlinear relationships between input and output datasets and

providing excellent prediction [24, 25]. One of the most used models is deep artificial neural networks (DANNs), which is considered a powerful method inspired by biological neural networks for solving problems such as function approximation, regression analysis, time series forecasting, classification analysis, and identification patterns in datasets, decision making, and data processing [26]. Compared to the most typical statistics, ANNs have shown various advantages, as they can handle several sorts of data, e.g., continuous, binomial, and discrete. Besides, they can develop complicated models without the need to previously know the functional dependency between several attributes, therefore, they can discover appropriate interconnections in the dataset. Furthermore, no specific experimental arrangement and a particular background are needed to apply ANNs; hence, they are easy to use and cost-effective techniques with fewer experimental runs for modelling procedures to produce the optimum findings [27, 28].

In this work, multi-layer perceptron ANNs are applied for the following causes first, they enable the artificial network to build parametrical nonlinear relationships of the input variables, as the output represents a nonlinear function of a linear combination of the neuron outputs in the hidden layer which themselves represent nonlinear functions of linear combinations of the input variables. Secondly, depending on the appealed response, the multi-layer perceptron ANNs automatically neglect some irrelevant factors by allocating zero or very small weights to these factors [26].

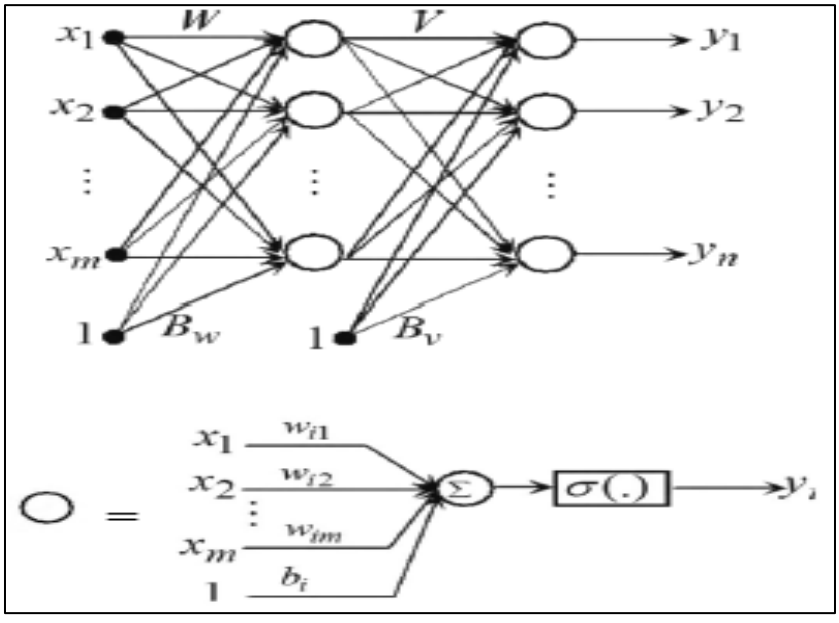

Figure 1: The schematic topography of the multi-layer perceptron ANNs [26].

The schematic topography of a multi-layer perceptron ANN is shown in Fig.1. In this network, the processing elements are the artificial neurons (nodes), which have layered structures and can receive information from other neurons or external inputs. Primarily, once an artificial neuron receives the input, which is weighted, it determines whether the output should be fed forward to the next layer as a response. Such a decision-making procedure is known as bias, and it is controlled through the activation function constructed into the network platform [29]. In addition, the weights in an artificial network correspond to the synapses in a biological neuron, whilst the activation function is analogous to the intracellular current conduction process in the soma. As can be seen in Fig.1, the output of the dependent variable (y) is a vector with n components defined by m components of an input vector of independent variables (x), as expressed in the following Equation (1)

$$y_i = \sum_{j=1}^{l}[v_{ij}g\left(\sum_{k=1}^{m} w_{jk}x_k + b_{wj}\right) + b_{vi}] \qquad (1)$$

Where v_{ij} and w_{jk} represent the synaptic weights, x_k is the input vector, g is an activation function, and b is the bias. It is well-known that the bias has a critical effect on the learning process by shifting the activation function to the left or right by increasing or decreasing the net input of the activation function, depending on whether it is positive or negative. In multilayer perceptron ANNs, the data is fed forwarded from input to output neurons through various hidden layers in only one direction with no back loops. It may also decrease the gradient error by adjusting weight and biases in non-linear models [29]. The structure of feed-forward ANNs in this work comprises four layers, which are one input layer with two nodes (frequency and temperature), one output layer with one node (the electrical conductivity) and two hidden layers with three neurons (see Fig. 2). The experimental input datasets were extracted from previously published literature [30, 31].

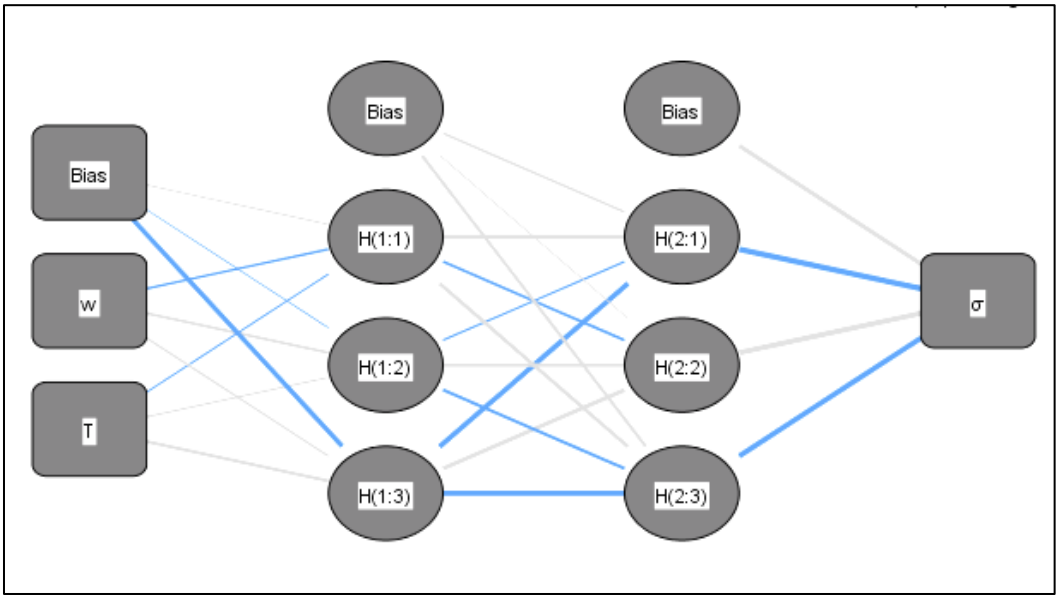

Figure 2: A basic diagram of ANN models.

In the multilayer perceptron ANNs, initializing the weights and threshold values, setting the numbers of hidden layers and neurons, and choosing the transfer function and the training algorithm are crucial factors in generating the desired output response. The rational steps of ANNs training process with supervised learning can be described as follows, generating sets of input and output patterns and initializing the weights (the connections between neurons) to random values. The activation is the next step, in which inputs and targets are applied, and the results of hidden and output layers are calculated in the forward direction where the information flows forward. The step of weight training is then applied, in which weights are adjusted by computing the error gradient, followed by the weights and biases updating using a learning algorithm. Similar steps are performed on the hidden layer in the backward direction, where the error calculated by the network is propagated backwards, and the weights are updated properly. Lastly, the iteration step is proceeded by repeating the procedure until the optimum response is accomplished. The steps of ANNs are demonstrated in Fig. 3.

The error algorithm can minimize a particular error by modifying the weights of the connections such an optimization process proceeds from left (output layer) to right in the back-propagation direction. The error function, which must be reduced, can be expressed as:

$$E = \frac{1}{2}\sum_{k=1}^{m}(a_k - t_k)^2 \qquad (2)$$

Where t_K and a_K represent the target values and network output, respectively. The E function depends on the weights, which change over time [32]. Another machine learning algorithm used in this work is a decision tree, which divides the dataset into binary tree topographies, where all datasets are nested under a root node and riven into several leaf nodes. In this model, each node is classified according to the cost function expressed as [33, 34, 35].

$$J(k, t_k) = \frac{m_L}{m} MSE_L + \frac{m_R}{m} MSE_R \quad (3)$$

Where k is the splitting feature, t_K is the threshold, MSE is the mean square error and m, m_L and m_R are the total number of training instances, left-node and right-node training instances, respectively. Furthermore, statistical indices were applied to determine the decision tree model's accuracy in predicting the electrical conductivity for organic-inorganic hybrid compounds, and the results are shown in Table. 1.

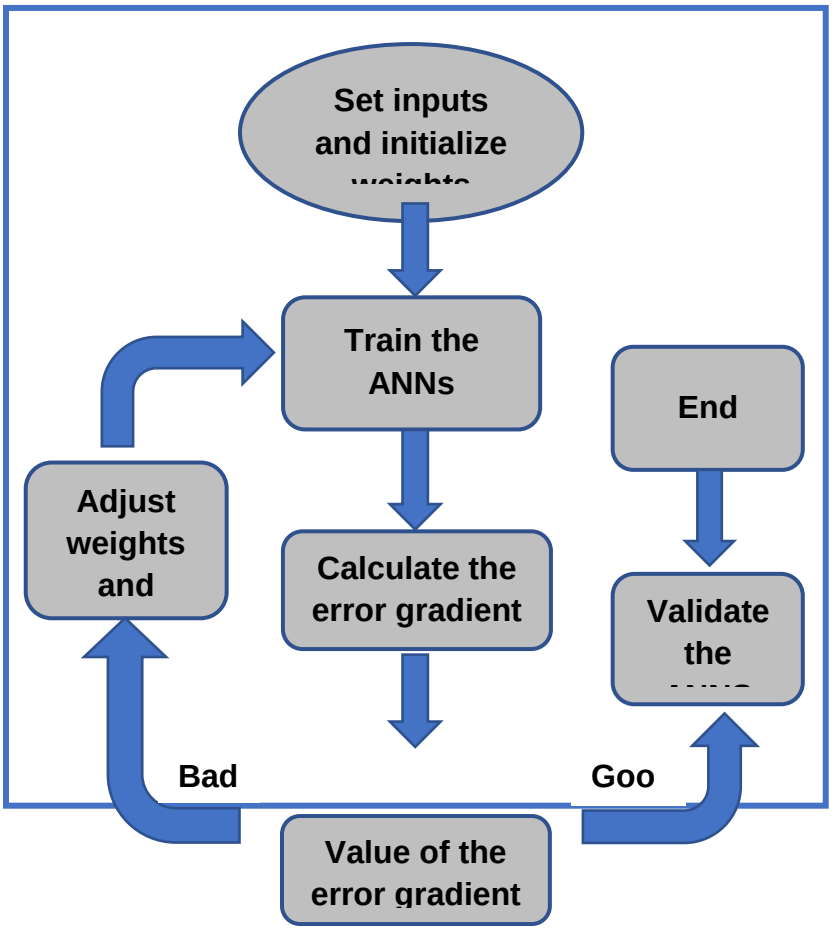

Figure 3: Logical steps of the ANNs training process.

Results and discussion

To find the best topology of ANNs which produces high performance, it is crucial to train the ANNs with different numbers of hidden layers, neurons, and activation functions using the experimental dataset in the generalization process. As mentioned previously, the optimum structure of ANNs applied in this research, which produces the lowest value of error gradient, consists of four layers, which are one input layer with two neurons, one output layer with one neuron, and two hidden layers with three neurons. These models were trained, tested, and validated in the datasets using the temperature and frequency as inputs with regard to the electrical conductivity as the output response. The training datasets were used to determine the weights and construct the network, whilst the testing datasets were applied to calculate errors and forbid overtraining effect through the training phase. To assess the model accuracy the electrical conductivity was predicted with the independent variables in the test dataset, and then the findings were compared with the targeted responses of the electrical conductivity in the test dataset. Usually, the input datasets are divided into two groups, training and testing, and when the output error is minimized, the training process stops. After adopting the ANN− SCG and ANN− GD models, it is better to understand the correlations between each feature of the inputs and the network simulated output, therefore the root mean squared error ($RMSE$), the correlation coefficient (R^2), and relative error (r) for all suggested algorithms measured as a criterion of model's performance using Equations (4), (5), and (6), respectively [36, 37].

$$RMSE = \sqrt{\frac{\sum_{i=1}^{n}(y_i-\hat{y}_i)^2}{n}} \quad (4)$$

$$R^2 = \left(\frac{\sum_{i=1}^{n}(y_i-\bar{y}_i)(\hat{y}_i-\bar{\hat{y}}_i)}{\sqrt{\sum_{i=1}^{n}(y_i-\bar{y}_i)^2}\sqrt{\sum_{i-1}^{n}(\hat{y}_i-\bar{\hat{y}}_i)^2}} \right)^2 \quad (5)$$

$$r = \left| \frac{Actual\ value_{out} - predicted\ value_{out}}{Actual\ value_{out}} \right| \times 100 \quad (6)$$

Where y_i and $\hat{y}_i$ are the targets and network outputs of the electrical conductivity, respectively, while $\bar{y}_i$ and , $\bar{\hat{y}}_i$ are the mean values of targeted and predicted electrical conductivity, respectively, and n is the total number of datasets.

Table1: The architectures of the proposed ANN models and their performance.

Compound	Optimization algorithm	Training hyperparameters	*RMSE* (Training)	*RMSE* (Testing)	Correlation coefficient (R^2)	Relative Error (r)
$[C_8H_{10}NO]_2[CdCl_4]$	ANN-SCG	Initial Lambda $=5\times10^{-7}$ Initial Sigma $=5\times10^{-5}$	0.027	0.007	0.99800	0.001
$[C_8H_{10}NO]_2[CdCl_4]$	ANN-GD	Initial Learning Rate=0.4 Momentum=0.9	0.032	0.035	0.99600	0.006
$[C_8H_{10}NO]_2[CdCl_4]$	ANN-GD	Initial Learning Rate=0.1 Momentum=0.5	0.041	0.039	0.99400	0.010
$[C_8H_{10}NO]_2[CdCl_4]$	ANN-GD	Initial Learning Rate=0.05 Momentum=0.3	0.037	0.056	0.99202	0.015
$[C_8H_{10}NO]_2[CdCl_4]$	Decision tree	—	2.423	—	0.863	—
$[(C_3H_7)_4N]_3Bi_3Cl_{12}$	ANN-SCG	Initial Lambda $=5\times10^{-7}$ Initial Sigma $=5\times10^{-5}$	0.045	0.022	0.99600	0.003
$[(C_3H_7)_4N]_3Bi_3Cl_{12}$	ANN-GD	Initial Learning Rate=0.4 Momentum=0.9	0.030	0.016	0.99814	0.002

$[(C_3H_7)_4N]_3$ Bi_3Cl_{12}	ANN-GD	Initial Learning Rate=0.1 Momentum=0.5	0.029	0.017	0.99809	0.002
$[(C_3H_7)_4N]_3$ Bi_3Cl_{12}	ANN-GD	Initial Learning Rate=0.05 Momentum=0.3	0.023	0.017	0.99821	0.003
$[(C_3H_7)_4N]_3$ Bi_3Cl_{12}	Decision tree	—	1.517	—	0.935	—

Table.1 demonstrates various predicted results using these statistical indicators for the proposed models. The *RMSE* is an effective metric for assisting the model efficiency when the errors are smoothly distributed across the data; it is always a positive value, and the optimal one should be zero. The more efficient a proposed model is in fitting a dataset, the lower the *RMSE*. Eight various ANN models were trained to predict the electrical conductivity for $[C_8H_{10}NO]_2[CdCl_4]$ and $[(C_3H_7)_4N]_3$ Bi_3Cl_{12}. As can be noticed from Table. 1, *RMSE* values of testing data range from 0.007 to 0.056 for $[C_8H_{10}NO]_2[CdCl_4]$, whilst their values of testing data vary between 0.016 and 0.022 for $[(C_3H_7)_4N]_3$ Bi_3Cl_{12}. On the other hand, the calculated *RMSE* of the decision tree algorithm was higher, which indicates a poor correlation between predicted and experimental datasets compared with the estimated values obtained from ANN models (see Table. 1).

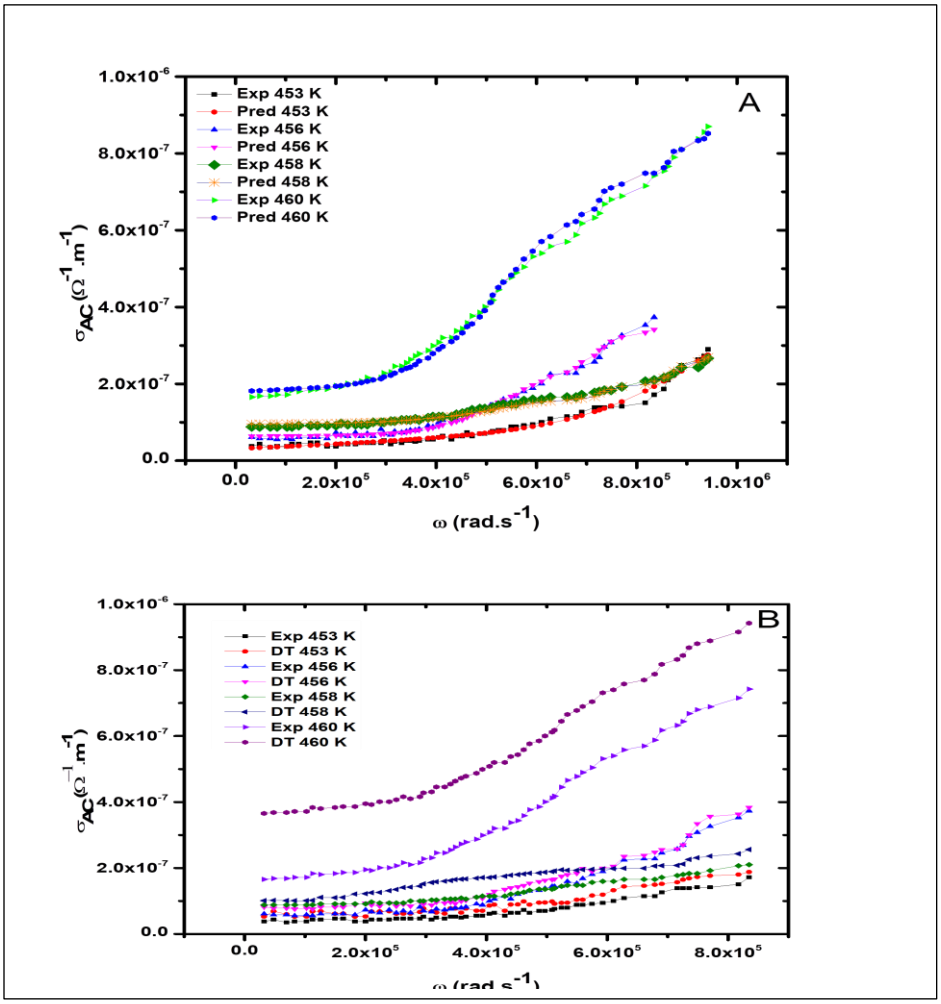

Figure 4: Frequency dependence of AC conductivity at several temperatures for $[C_8H_{10}NO]_2[CdCl_4]$ using (**A**) ANNs and (**B**) decision tree algorithm, respectively.

In addition, after the training of ANNs and decision tree algorithms, the targeted datasets and predicted outputs of the electrical conductivity of $[C_8H_{10}NO]_2[CdCl_4]$ in terms of temperature and frequency were compared. The predicted results obtained from ANN models and decision tree algorithms are shown in Fig. 4 (A) and (B), respectively.

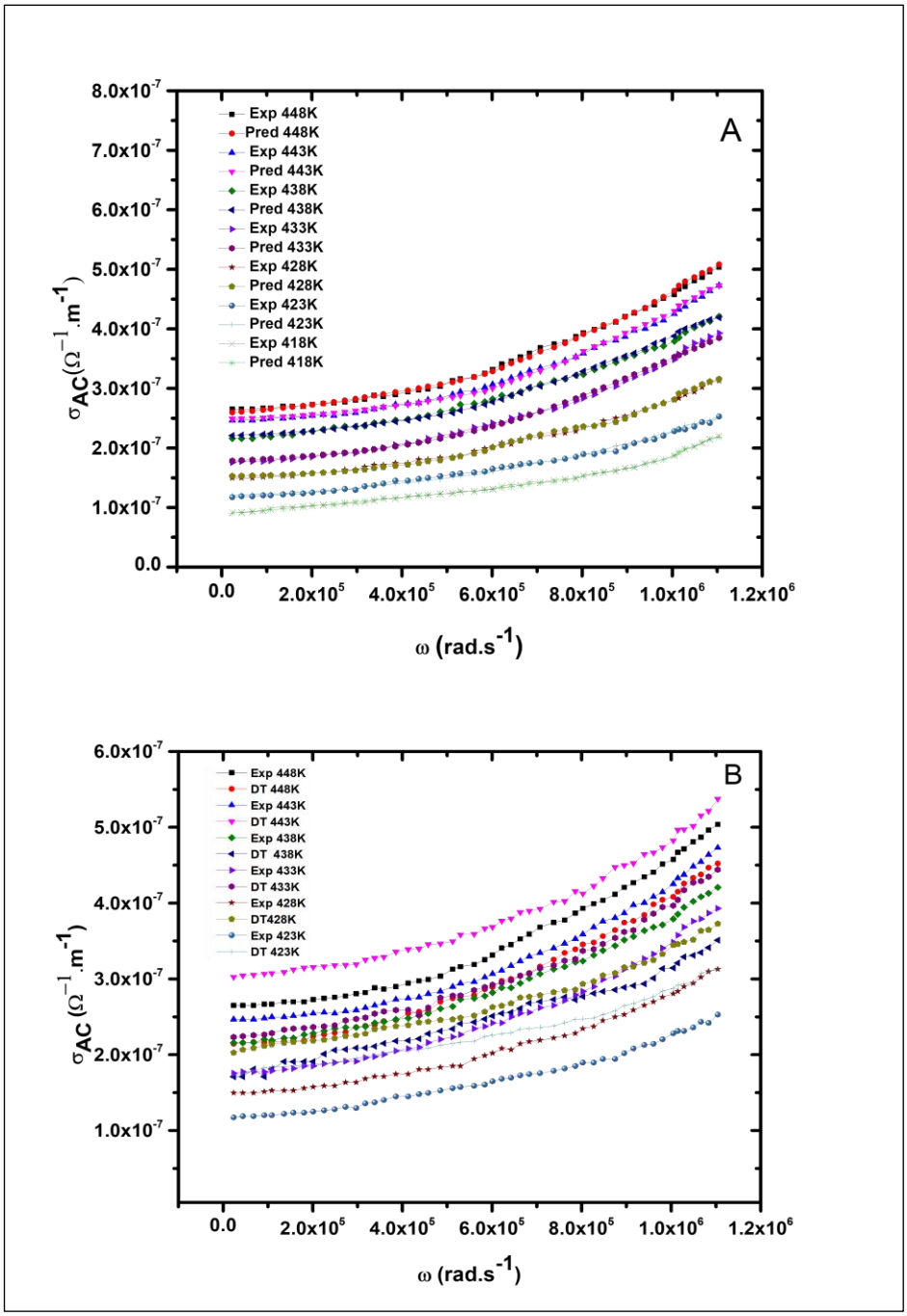

Figure 5: Frequency dependence of AC conductivity at several temperatures for $[(C_3H_7)_4N]_3Bi_3Cl_{12}$ using (**A**) ANNs and (**B**) decision tree algorithm, respectively.

It can be shown from Fig. 4 (A) that ANN models can adequately demonstrate the relationships between the electrical conductivity and the input parameters. Besides, the ANNs predicted

values are closer to the experimental ones, indicating that these models are powerful techniques to simulate the electrical properties for electrical and electronics engineering applications. In contrast, the estimated findings produced by the decision tree model showed that this algorithm is less accurate in anticipating the electrical conductivity for organic–inorganic hybrid compounds and did not deliver promising performance (see Fig. 4 (B)). Furthermore, the electrical conductivity in terms of temperature and frequency for $[(C_3H_7)_4N]_3\,Bi_3Cl_{12}$ using ANNs and decision tree algorithms are illustrated in Fig. 5 (A) and (B), respectively. It can be shown that the predicted findings resulting from ANNs are considerably fitter than those of the decision tree model. Besides, ANNs' predicted results showed excellent accuracy with lower *RMSE* values than those calculated by the decision tree algorithm. It is essential to visualize the *RMSE* error of the input datasets through a histogram plot, which is one of the most used plots of the ANN models. In general, the error histogram shows how the errors from the testing datasets are distributed, in other words, it describes how simulated results diverge from the target ones by determining the level of noise in the input datasets. Therefore, based on the error histogram distribution, it can be assured that the average error in the datasets is in a reasonable range. The histogram of errors generated by ANNs through predicting the electrical conductivity for organic–inorganic hybrid materials is demonstrated in Fig. 6. As can be shown, the majority of data sets were distributed around zero, which indicates the validation of the input datasets for each predicted output.

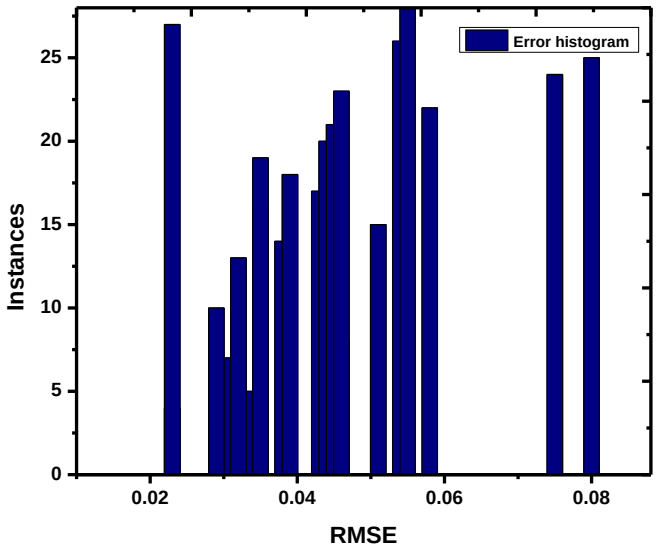

Figure 6: The histogram of the estimated *RMSE*.

In addition, the criterion of efficiency for the proposed models was evaluated using the correlation coefficient (R^2). In general, the correlation coefficient indicates how accurately the predicted values of models closely fit or fit the targeted ones, and further satisfactorily and highest magnitude denotes a highly fitted model with a strong correlation between the predicted and targeted data sets. The accuracy of the ANNs and decision tree models in terms of the correlation coefficient is illustrated in Table. 1. It is observed that the ANNs algorithms have the most creditability with higher R^2 values of 0.998 and 0.996 and lower values of the relative error (r) of 0.001 and 0.002, which are consistent with the obtained results demonstrated in Fig. 4 and 5. On the other hand, the decision tree models were less capable of simulating the electrical conductivity values with considerable accuracies in terms of higher *RMSE* values of 2.423 and lower R^2 values of 0.863. Based on these results, it seems that the ANN models were more credible and efficient in evaluating the electrical conductivity of organic–inorganic hybrid compounds. Besides, they proved a good correlation between the independent variables and the network output, whilst the decision tree algorithm showed less prediction accuracy.

Conclusion

In the current research, a proposed analytical methodology to apply different predictive artificial intelligence algorithms, including ANN-SCG, ANN-GD and decision tree, was carried out for predicting the electrical conductivity of organic–inorganic hybrid compounds. It aimed to determine the most efficient anticipative algorithms, which can generate the most applicable and stable output response through different groups of independent input parameters. The high correlation coefficient between the simulated and experimental electrical conductivity, the low prediction *RMSE* and relative error show that the high performance of the ANNs, as computational intelligence approaches, for modelling and understanding the relationship between the electrical properties of organic–inorganic materials, as a function of frequency and temperature. On the other hand, the decision tree algorithm has a low correlation coefficient and high *RMSE* values, indicating that it was less efficient in achieving the desired performance compared to ANN models. In addition, the training methodology adopted in this paper is not only exclusive to solid–solid platforms, as other heterostructures like solid–liquid materials could be considered using these types of artificial intelligence techniques. Besides, the most essential impacting parameters should be selected as training inputs using the ANNs simulations to achieve high performance and precision.

References

[1] Li, X., Pan, F., Sun, C., Zhang, M., Wang, Z., Du, J., Wang, J., Xiao, M., Xue, L., Zhang, Z.G. and Zhang, C., 2019. Simplified synthetic routes for low cost and high photovoltaic performance n-type organic semiconductor acceptors. *Nature communications*, *10*(1), p.519.

[2] Yamamura, A., Watanabe, S., Uno, M., Mitani, M., Mitsui, C., Tsurumi, J., Isahaya, N., Kanaoka, Y., Okamoto, T. and Takeya, J., 2018. Wafer-scale, layer-controlled organic single crystals for high-speed circuit operation. *Science advances*, *4*(2), p.eaao5758.

[3] Wang, Q., Qian, J., Li, Y., Zhang, Y., He, D., Jiang, S., Wang, Y., Wang, X., Pan, L., Wang, J. and Wang, X., 2016. 2D single-crystalline molecular semiconductors with precise layer definition achieved by floating-coffee-ring-driven assembly. *Advanced Functional Materials*, *26*(19), pp.3191-3198.

[4] Park, S.H.K., Ryu, M., Hwang, C.S., Yang, S., Byun, C., Lee, J.I., Shin, J., Yoon, S.M., Chu, H.Y., Cho, K.I. and Lee, K., 2008, May. 42.3: Transparent ZnO thin film transistor for the application of high aperture ratio bottom emission AM-OLED display. In *SID Symposium Digest of Technical Papers* (Vol. 39, No. 1, pp. 629-632). Oxford, UK: Blackwell Publishing Ltd.

[5] Geffroy, B., Le Roy, P. and Prat, C., 2006. Organic light-emitting diode (OLED) technology: materials, devices and display technologies. *Polymer international*, *55*(6), pp.572-582.

[6] Chow, P.C. and Someya, T., 2020. Organic photodetectors for next-generation wearable electronics. *Advanced Materials*, *32*(15), p.1902045.

[7] Muccini, M., 2006. A bright future for organic field-effect transistors. *Nature materials*, *5*(8), pp.605-613.

[8] Sirringhaus, H., 2014. 25th anniversary article: organic field-effect transistors: the path beyond amorphous silicon. *Advanced materials*, *26*(9), pp.1319-1335.

[9] Yang, J., Yan, D. and Jones, T.S., 2015. Molecular template growth and its applications in organic electronics and optoelectronics. *Chemical reviews*, *115*(11), pp.5570-5603.

[10] Khan, J., Ahmad, R.T.M., Tan, J., Zhang, R., Khan, U. and Liu, B., 2023. Recent advances in 2D organic– inorganic heterostructures for electronics and optoelectronics. *SmartMat*, *4*(2), p.e1156.

[11] Jariwala, D., Howell, S.L., Chen, K.S., Kang, J., Sangwan, V.K., Filippone, S.A., Turrisi, R., Marks, T.J., Lauhon, L.J. and Hersam, M.C., 2016. Hybrid, gate-tunable, van der Waals p–n heterojunctions from pentacene and MoS2. *Nano letters*, *16*(1), pp.497-503.

[12] Huang, F., Li, J.Z., Xu, Z.H., Liu, Y., Luo, R.P., Zhang, S.W., Nie, P.B., Lv, Y.F., Zhao, S.X., Su, W.T. and Li, W.D., 2019. A bilayer 2D-WS2/organic-based heterojunction for high-performance photodetectors. *Nanomaterials*, *9*(9), p.1312.

[13] Sun, M., Yang, P., Xie, D., Sun, Y., Xu, J., Ren, T. and Zhang, Y., 2019. Self-Powered MoS2–PDPP3T heterotransistor-based broadband photodetectors. *Advanced Electronic Materials*, *5*(2), p.1800580.

[14] Pepels, M., Filot, I., Klumperman, B. and Goossens, H., 2013. Self-healing systems based on disulfide–thiol exchange reactions. *Polymer Chemistry*, *4*(18), pp.4955-4965.7

[15] Feng, S., Tan, J., Zhao, S., Zhang, S., Khan, U., Tang, L., Zou, X., Lin, J., Cheng, H.M. and Liu, B., 2020. Synthesis of ultrahigh-quality monolayer molybdenum disulfide through in situ defect healing with thiol molecules. *Small*, *16*(35), p.2003357.

[16] Stylianakis, M.M., Konios, D., Petridis, C., Kakavelakis, G., Stratakis, E. and Kymakis, E., 2017. Ternary solution-processed organic solar cells incorporating 2D materials. *2D Materials*, *4*(4), p.042005.

[17] Ricciardulli, A.G. and Blom, P.W., 2020. Solution-processable 2D materials applied in light-emitting diodes and solar cells. *Advanced Materials Technologies*, *5*(8), p.1900972.

[18] Zhang, L., Sharma, A., Zhu, Y., Zhang, Y., Wang, B., Dong, M., Nguyen, H.T., Wang, Z., Wen, B., Cao, Y. and Liu, B., 2018. Efficient and layer-dependent exciton pumping across atomically thin organic–inorganic type-I heterostructures. *Advanced Materials*, *30*(40), p.1803986.

[19] Futscher, M.H., Schultz, T., Frisch, J., Ralaiarisoa, M., Metwalli, E., Nardi, M.V., Müller-Buschbaum, P. and Koch, N., 2018. Electronic properties of hybrid organic/inorganic semiconductor pn-junctions. *Journal of Physics: Condensed Matter*, *31*(6), p.064002.

[20] Presolski, S., Wang, L., Loo, A.H., Ambrosi, A., Lazar, P., Ranc, V., Otyepka, M., Zboril, R., Tomanec, O., Ugolotti, J. and Sofer, Z., 2017. Functional nanosheet synthons by covalent modification of transition-metal dichalcogenides. *Chemistry of Materials*, *29*(5), pp.2066-2073.

[21] Niu, L., Li, K., Zhen, H., Chui, Y.S., Zhang, W., Yan, F. and Zheng, Z., 2014. Salt-assisted high-throughput synthesis of single-and few-layer transition metal dichalcogenides and their application in organic solar cells. *Small (Weinheim an der Bergstrasse, Germany)*, *10*(22), pp.4651-4657.

[22] Ling, H., Koutsouras, D.A., Kazemzadeh, S., Van De Burgt, Y., Yan, F. and Gkoupidenis, P., 2020. Electrolyte-gated transistors for synaptic electronics, neuromorphic computing, and adaptable biointerfacing. *Applied Physics Reviews*, *7*(1).

[23] Okutan, M., Basaran, E., Bakan, H.I. and Yakuphanoglu, F., 2005. AC conductivity and dielectric properties of Co-doped TiO2. *Physica B: Condensed Matter*, *364*(1-4), pp.300-305.

[24] Gago, J., Martínez-Núñez, L., Landín, M. and Gallego, P.P., 2010. Artificial neural networks as an alternative to the traditional statistical methodology in plant research. *Journal of plant physiology*, *167*(1), pp.23-27.

[25] Landín, M., Rowe, R.C. and York, P., 2009. Advantages of neurofuzzy logic against conventional experimental design and statistical analysis in studying and developing direct compression formulations. *European Journal of Pharmaceutical Sciences*, *38*(4), pp.325-331.

[26] Suzuki, K. ed., 2011. *Artificial neural networks: methodological advances and biomedical applications*. BoD–Books on Demand.

[27] Colbourn, E., 2003. Neural Computing Enables Intelligent Formulations. *Pharmaceutical Technology*, *18*, pp.16-21.

[28] Colbourn, E. and Rowe, R.C., 2005. Neural computing and pharmaceutical formulation. *Encyclopaedia of pharmaceutical technology*.

[29] Kalantary, S., Jahani, A. and Jahani, R., 2020. MLR and Ann approaches for prediction of synthetic/natural nanofibers diameter in the environmental and medical applications. *Scientific reports*, *10*(1), p.8117.

[30] Trigui, W., Oueslati, A., Chaabane, I. and Hlel, F., 2014. Synthesis, crystal structure, dielectric properties, and AC conductivity of tri-tetrapropylammonium dodeca chlorobismuthate (III). *Ionics*, *20*, pp.231-241.

[31] Jellibi, A., Chaabane, I. and Guidara, K., 2016. Experimental and theoretical study of AC electrical conduction mechanisms of Organic–inorganic hybrid compound Bis (4-acetylanilinium) tetrachlorocadmiate (II). *Physica E: Low-dimensional Systems and Nanostructures*, *80*, pp.155-162.

[32] Li, J., 2008. Computational analysis of nanofluid flow in microchannels with applications to micro-heat sinks and bio-MEMS.

[33] Quinlan, J.R., 1987. Simplifying decision trees. *International journal of man-machine studies*, *27*(3), pp.221-234.

[34] Breslow, L.A. and Aha, D.W., 1997. Simplifying decision trees: A survey. *Knowledge engineering review*, *12*(1), pp.1-40.

[35] Quinlan, J.R., 1999. Simplifying decision trees. *International Journal of Human-Computer Studies*, *51*(2), pp.497-510.

[36] Helaleh, A.H. and Alizadeh, M., 2016. Performance prediction model of miscible surfactant-CO2 displacement in porous media using support vector machine regression with parameters selected by ant colony optimization. *Journal of Natural Gas Science and Engineering*, *30*, pp.388-404.

[37] Otchere, D.A. ed., 2024. *Data Science and Machine Learning Applications in Subsurface Engineering*. CRC Press, Taylor & Francis Group.